General Disclaimer

One or more of the Following Statements may affect this Document

- This document has been reproduced from the best copy furnished by the organizational source. It is being released in the interest of making available as much information as possible.

- This document may contain data, which exceeds the sheet parameters. It was furnished in this condition by the organizational source and is the best copy available.

- This document may contain tone-on-tone or color graphs, charts and/or pictures, which have been reproduced in black and white.

- This document is paginated as submitted by the original source.

- Portions of this document are not fully legible due to the historical nature of some of the material. However, it is the best reproduction available from the original submission.

DEPARTMENT OF SPACE SCIENCE & APPLIED PHYSICS

The Catholic University of America
Washington, D.C. 20017

NATIONAL AERONAUTICS AND SPACE ADMINISTRATION

Research Grant NGR-09-005-025

Diagnostics of Accelerating Plasma

5th Semi-Annual Progress Report

March 1, 1968 - Aug. 31, 1968

Report No. 68-011

by

T.N. Lie and K.F. Lee

and

E.A. McLean

Dec. 1, 1968

Department of Space Science and Applied Physics
The Catholic University of America
Washington, D.C.

Foreword

The present semi-annual progress report consists of two separate studies, i.e., 1) Laser Scattering Experiment with Magnetically Driven Shock Tube, 2) Drift Instabilities in Two-Component Plasmas. The former study was presented at APS Plasma Physics Meeting at Miami Beach, Fla., on Nov. 13-16 and the latter which is the work by K.F. Lee has been published in Journal of Applied Physics, 39 3861 (1968). We wish to acknowledge the contribution made to this report by M.J. Rhee, a graduate assistant.

ABSTRACT

The electron temperatures and densities behind the incident and reflected shock front in the T-type electromagnetic shock tube are determined using the LASER light scattering method. Since this method only depends on the assumption of the Maxwelliam velocity distribution of the plasma particles, the electron temperatures thus obtained are independent of the local thermal equilibrium assumption in the plasma. The laser scattering temperatures are then compared with the spectroscopic temperature which depends on LTE condition. It was found that the two temperature well agree within the experimental uncertainty indicating that the LTE assumption in the spectroscopic temperature determination is a reasonable approximation.

As a preliminary study for the coaxial plasma accelerator, the stability of a plasma having two components of different drift velocities and temperatures and bounded by a conducting cylinder is investigated. General expressions are given for the velocity thresholds, maximum unstable wavenumber, and the number of unstable modes in a system. In conjunction with the geometrical parameters given earlier, the formulas can be used to study streaming instabilities under a variety of conditions. It is seen that the instability depends sensitively on both the geometry and the temperature ratio of the two components.

TABLE OF CONTENTS

LIST OF ILLUSTRATION

Tables

I. Laser Scattering Experiment with Magnetically Driven Shock Tube

A. Introduction

Our previous diagnostics of coaxial accelerator plasmas have been made mainly by spectroscopic methods. The spectroscopic methods have often proved to provide a convenient and accurate measurement of plasma parameters without disturbing the plasma. However, the determination of some parameters such as the plasma temperature often heavily depends on an assumption of the local thermal equilibrium (LTE) condition in the plasmas. During the last few years, there has been considerable discussions in the literature[1,2,3] concerning whether the condition of LTE is fulfilled in electromagnetically driven shock tubes such as the T-tube and the coaxial plasma accelerator. Eckerle and McWhirter[3] reported that the LTE condition does not exist in a T-tube containing a 99 percent H_2 and 1 percent H_e mixture. The reason for the departure from LTE was shown to be the rapid rate of change of the plasma conditions. Figure 1 illustrates their result, where the electron density and the temperatures are plotted against time. One sees that the two temperature determinations, one from the Balmer discontinuity method which does not depend on the LTE assumption and the temperature obtained by the line intensity ratio of He II 4686 and He I 5876 which depends on the LTE assumption, do not agree and that a factor of two difference exists at the peak electron density. According to a criteria given by Griem[4] for the complete LTE between the ground state and excited states of singly ionized helium in this transient plasma of 4 eV, the electron density of $10^{18} cm^{-3}$ or greater is required. Recently, it is shown[5] that the LTE assumption is in fact a satisfactory approximation in a coaxial accelerator plasma where the electron density and the temperature are comparable to that in a T-tube, i.e., $N_e \sim 10^{17} cm^{-3}$ and $T_e \sim 4$ eV. However, a

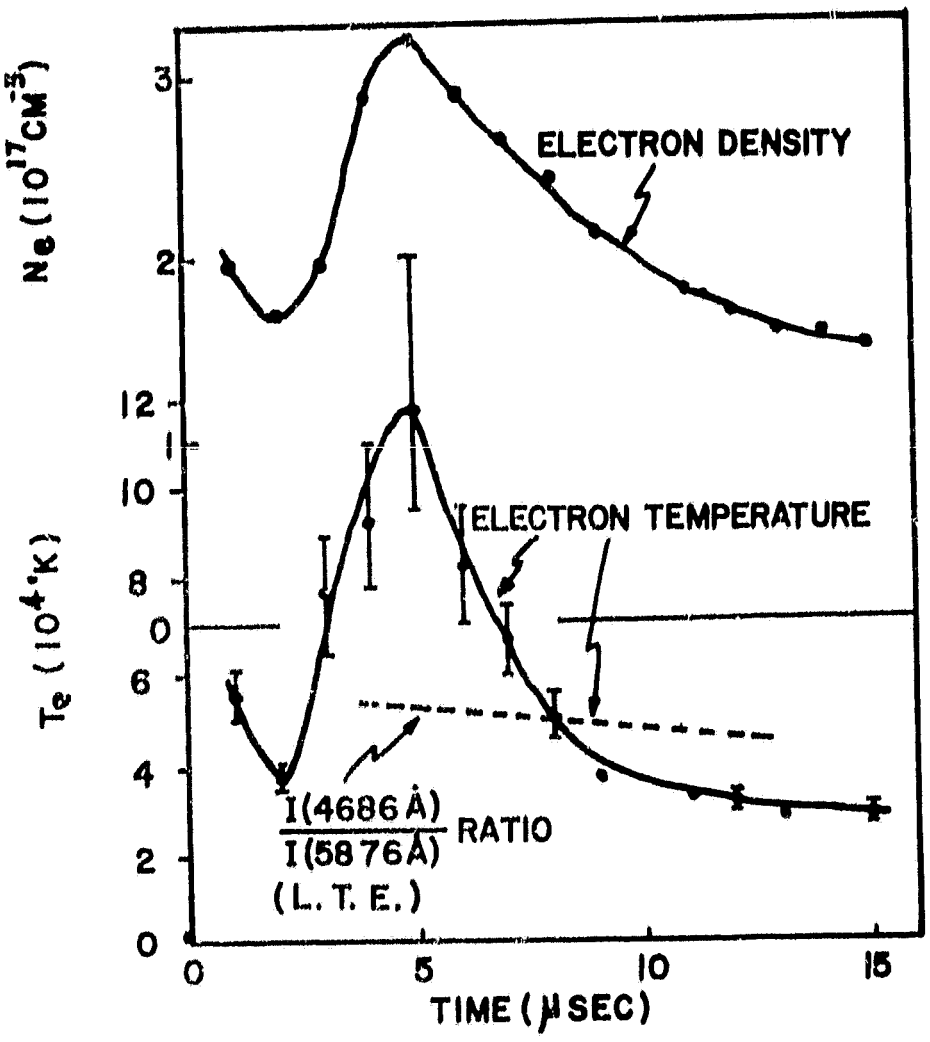

FIG. 1 ELECTRON TEMPERATURE AND DENSITY AGAINST TIME (FROM REFERENCE 3)

clear-cut experimental verification is required in order to clarify the situation. In the present investigation, the electron temperature and density behind the incident and reflected shock in a T-tube are determined using both laser light scattering method, which is independent of the LTE assumption, and a spectroscopic technique, i.e., line intensity ratio of He II 4686 and He I 5876. It is found that the two temperatures thus obtained agree well, within the experimental uncertainty, indicating that at least an approximate LTE condition exists in this kind of a transient plasma. It is also noted that the laser scattering method is an excellent diagnostic technique which gives accurate values of the plasma parameters, with both time and space resolution. The T-tube plasma is used for the diagnostics in this experiment because it has simple geometry and provides easy determination of spectroscopic temperature and density, however the method will be extended further to the other type of plasma accelerators to determine such parameters as T_e, N_e, T_i and the neutral particle density (Rayleigh scattering).

B. Experimental Arrangement

A schematic diagram of the experimental set-up is shown in Figure 2. A T-tube with a side arm 12 cm long is used. The diameter of the tube is about 2.5 cm. The electrodes are connected to 2.2 μf capacitor through a spark gap switch. The charging voltage of the capacitor is fixed to 15 kV and the ringing frequency of the discharge is 250 kH_z. The gas used is helium or hydrogen at filling pressures of 1 Torr and 1/2 Torr. All the optical observations were made at a position 3 mm behind the end of the side arm either with or without a reflector disc located 6 mm beyond the end of the side arm.

To make the 90 degree LASER scattering measurements, a Q-switched (pockel cell) ruby LASER is directed perpendicular to the T-tube side arm. The laser beam is focused

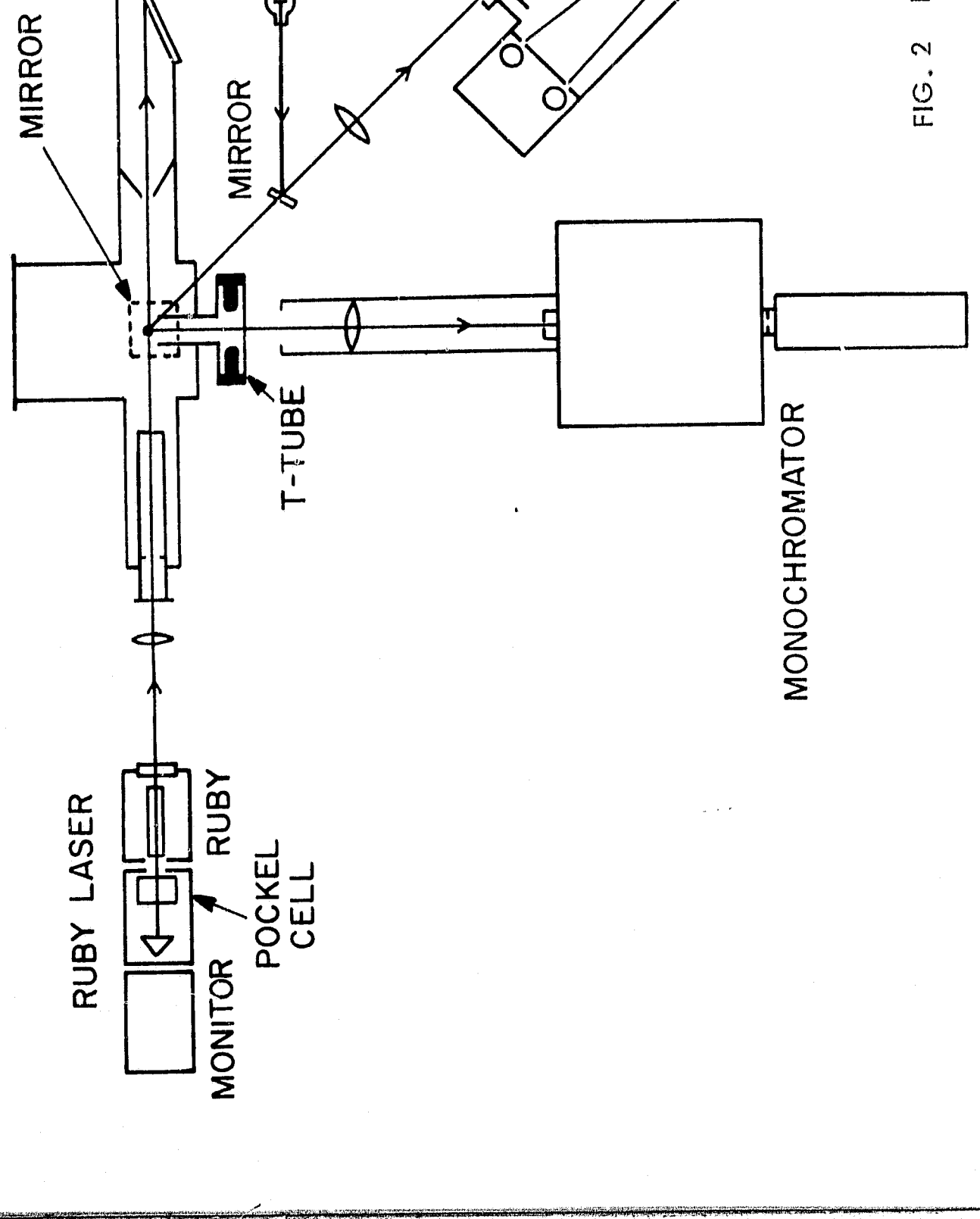

FIG. 2 EXPERIMENTAL ARRANGEMENT

to a spot about 1 mm in diameter at the center of the T-tube side arm and at 3 mm from the end of the side arm. The synchronization of the LASER pulse is made using a directed light guide and a delay generator. The spectral observations of the scattered laser light are made perpendicular to the plane of the diagram using a mirror to deflect the scattered light into a monochromator (with S-20 response photomultiplier tube). The laser pulse output is monitored shot-to-shot with a photodiode which is calibrated previously using a calorimeter. The duration of the laser pulse is about 20 nanoseconds and the total energy in a laser pulse is 2-3 joules. The stray light of the laser from the walls of the system is practically eliminated by use of a number of diaphragms, baffles and the beam dump Brewster angle window with the absorber as shown in the diagram.

Simultaneously with the laser scattering measurements, observations of the spectral line intensities of He II 4686 and He I 5876 were made at the same position of the T-tube using a polychromator. The polychromator is calibrated against wavelength using a standard tungsten ribbon filament lamp.

C. Results

If laser radiation is incident on a plasma blob, a certain amount of the light is scattered into a particular angle θ. The amount of momentum transferred to the incident photon is $\bar{p} = \hbar\bar{k}_p$ and can be supplied either by a single electron or by longitudinal plasma oscillations. These two regimes are characterized by the parameter

$$\alpha = \frac{\lambda_0}{4\pi\lambda_D \sin\frac{\theta}{2}} = \frac{1}{2\pi}\frac{k_D}{k_p}$$

where $k_D = \frac{2\pi}{\lambda_D}$, $\lambda_D = \left[\frac{kT_e}{4\pi N_e e^2}\right]^{\frac{1}{2}}$ and $k_p = 2k_o \sin\frac{\theta}{2}$.

If the momentum transfer is small compared to the momentum associated with the plasma waves, $\alpha >> 1$. Conversely, when the momentum transferred to the incident wave is large compared to the momentum associated with the plasma oscillations, $\alpha << 1$. Therefore, the spectral distribution of the scattered radiation into a certain angle is characterized by α. The complete spectrum of the scattered radiation for typical laboratory plasmas have been calculated by a number of investigators[6,7]. In the present work we make use of calculated set of graphs reported by W.H. Kegel[7]. The graphs represent spectra of 90 degree scattering from a plasma of $T_e = 100,000^{\circ}K$ and α as variable parameter. The electron density and temperature are then determined by comparing the experimentally obtained spectral profile with these calculated profiles. The spectral distributions of the scattered laser radiations are measured on shot-to-shot basis assuming reproducibility of the T-tube. It is required to fire the laser at the desired moment within an accuracy of ~ 0.1 μsec due to the very rapid change in N_e behind the shock. It is rather difficult to achieve this with the present system because of the non-reproducible light pick-up by the light guide. However, this problem is solved by selecting only the recorded data which occur at the right moment. A typical oscillogram of the scattered laser light superimposed with plasma continuum and the laser power monitor signal from the photodiode is shown in Figure 3. Figures 4, 5 and 6 illustrate observed profiles of scattered radiation in the case of an incident shock wave (H_e at $p = 1$ Torr) at various instances of time. The solid curves are the best fit to the calculated curves taken from the report by Kegel. Also shown in Figure 5 is the profile which would be given by a plasma with the same density but a temperature of 9 eV or about 2 times the spectroscopic temperature, one notes

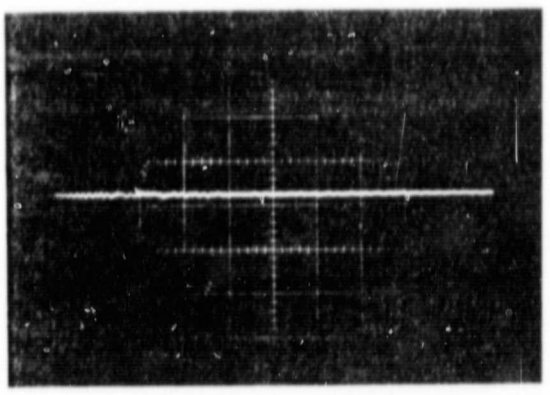

0.1 μsec/div

(a)

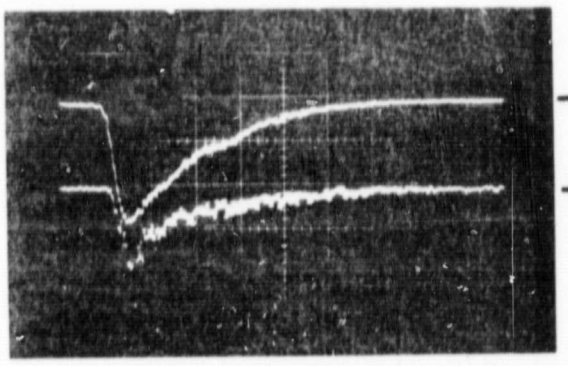

0.5 μsec/div

(b)

FIG. 3 TYPICAL PHOTOELECTRIC RECORDINGS OF (a) LASER PULSE SIGNAL FROM THE PHOTODIODE and (b) He II 4686 and SCATTERED LASER SIGNAL

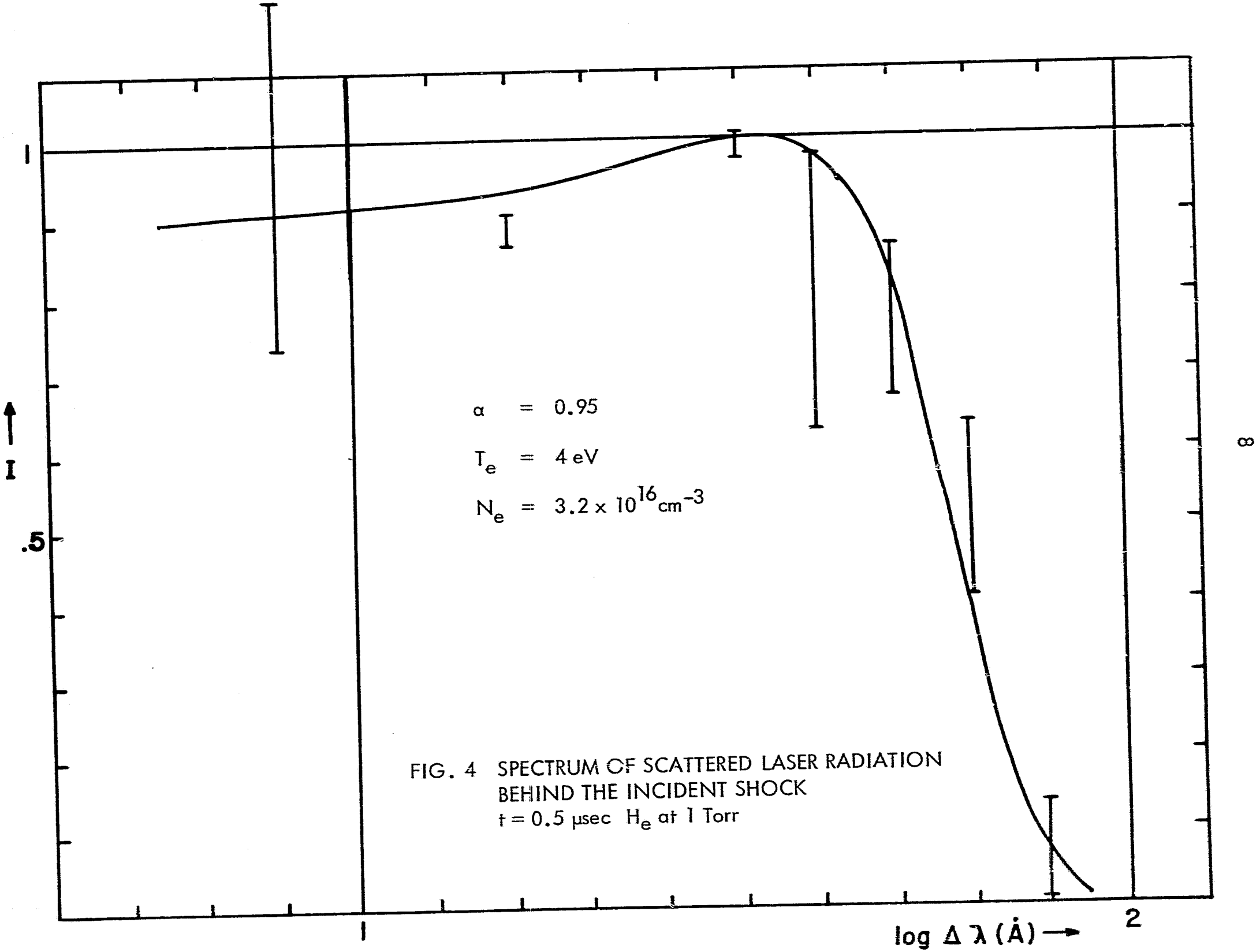

FIG. 4 SPECTRUM OF SCATTERED LASER RADIATION BEHIND THE INCIDENT SHOCK
$t = 0.5$ μsec H_e at 1 Torr

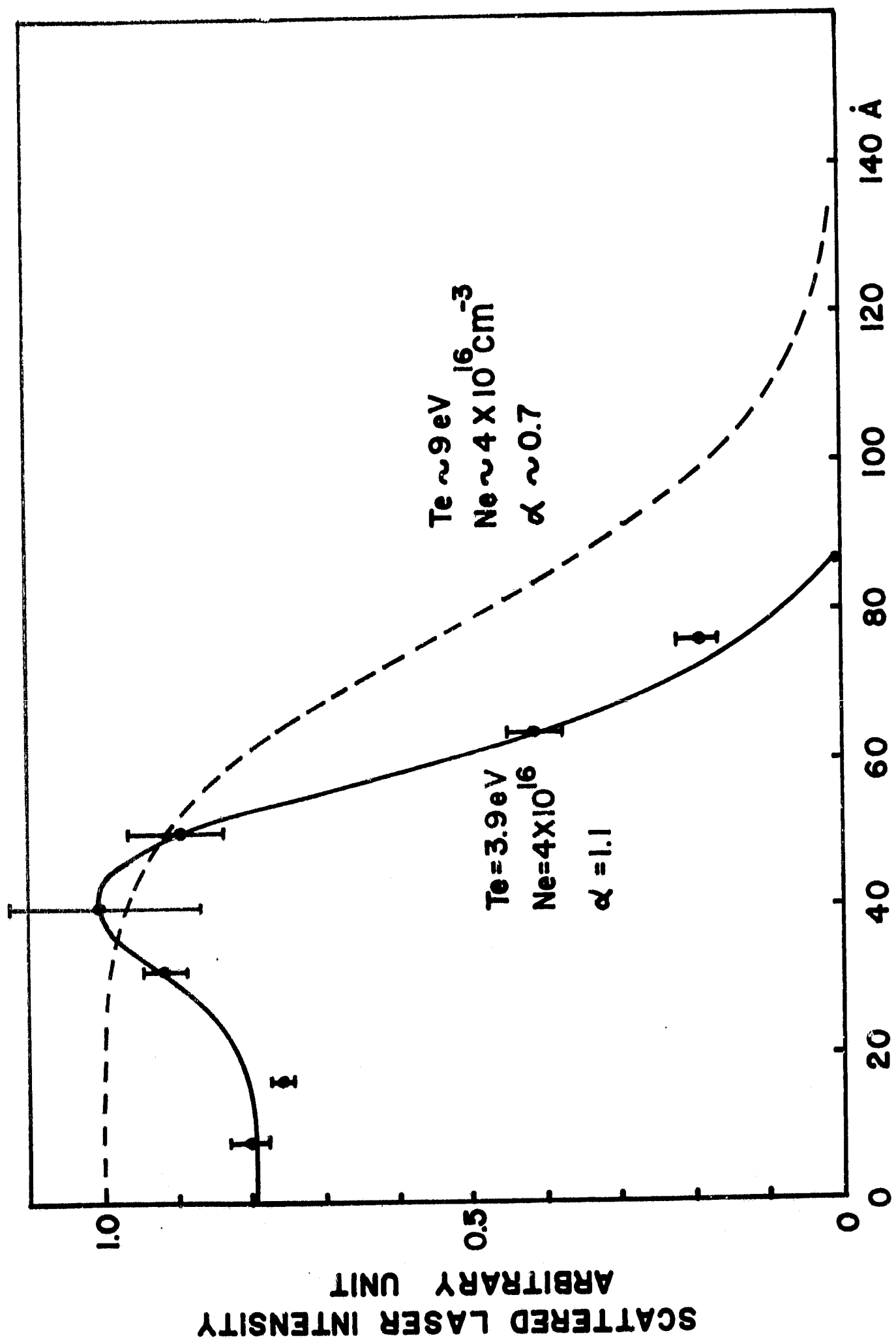

FIG. 5 SPECTRUM OF SCATTERED LASER RADIATION BEHIND THE INCIDENT SHOCK AT t = 1.0 μsec, H_e at 1 TORR

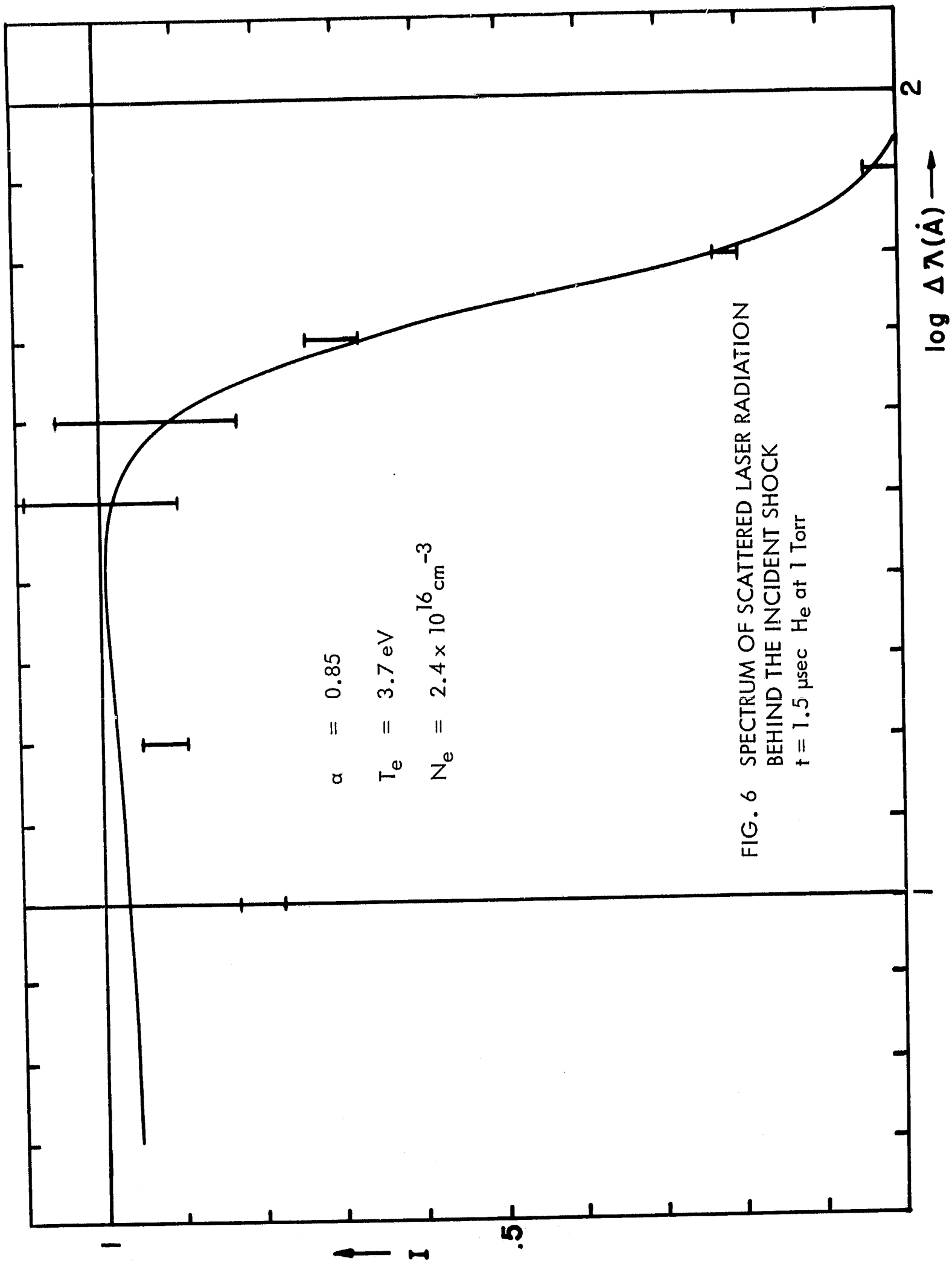

FIG. 6 SPECTRUM OF SCATTERED LASER RADIATION
BEHIND THE INCIDENT SHOCK
t = 1.5 μsec H_e at 1 Torr

that the 9 eV curve falls well outside of the error brackets of the experimental data. Figure 7 gives a summary of the values of temperature and density behind the shock obtained by the laser scattering technique and the temperature obtained from the line intensity ratio of He II 4686 and He I 5876. One sees that the spectroscopic temperatures are consistently lower than the values obtained from laser scattering; however, they do agree within the estimated error.

The same scattering experiment is extended to the reflected shock of the T-tube by placing a reflector disc at 6 mm beyond the end of the tube. The filling gas is helium at 0.5 Torr. Figure 8 shows a typical photoelectric signal of continuum radiation at the laser frequency (6980 $\mathring{A}$). Figures 9 and 10 again show the scattered laser intensity plotted againste $\log(\Delta\lambda)$ and the calculated curves. Here the characteristic parameter α is 1.85 and 1.50 respectively. Measured values of T_e and N_e obtained both by laser scattering and the spectroscopic method are shown in Figure 11 with the time history of the N_e and T_e. For this case, $N_e \sim 1.4 \times 10^{17} cm^{-3}$ and one again sees a similar agreement between the two temperatures. Hydrogen gas is used as a filling gas at p = 0.5 Torr in order to compare the result with that of Eckerle and McWhirter[3]. The profile is shown in Figure 12, and the measured laser scattering temperature and density immediately behind the shock frong (0.1 μsec from the density peak) are T_e = 4.6 eV ± 10 percent and $N_e = 1.7 \times 10^{17} cm^{-3}$, respectively.

Although the difference between the laser scattering and the spectroscopic temperature is about the same as the estimated error, the deviation between the two could be due to (1) the departure from the LTE in the plasma, or (2) the inhomogeneity in temperature along the line of sight for the He II 4686/He I 5876 measurement. The former explanation

	LASER SCATTERING		SPECTROSCOPIC
	Te	Ne	Te
0.5 μsec	4.0eV (±10%)	$3.2\times10^{16}cm^{-3}$ (±10%)	3.5 eV (±15%)
1.0 "	3.9 "	4.0 "	3.3 "
1.5 "	3.7 "	2.4 "	3.2 "
2.0 "	3.4 "	2.2 "	

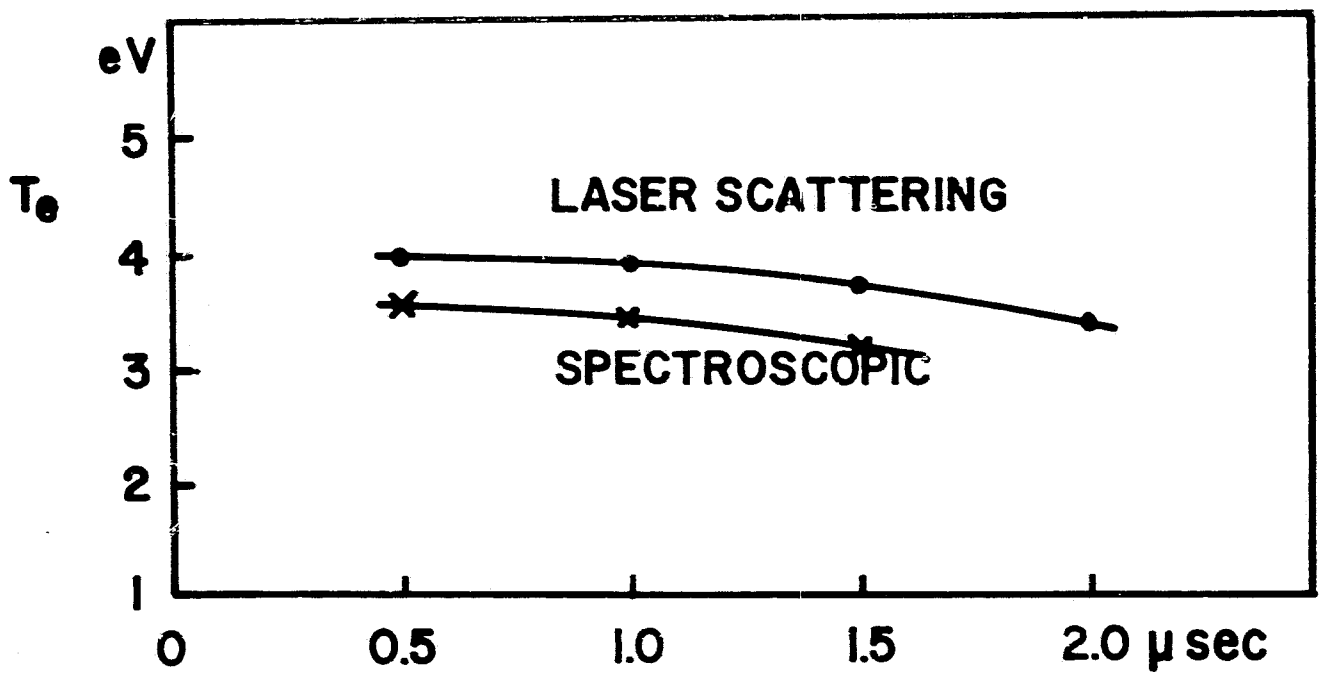

FIG. 7 ELECTRON DENSITY AND TEMPERATURE BEHIND THE INCIDENT SHOCK

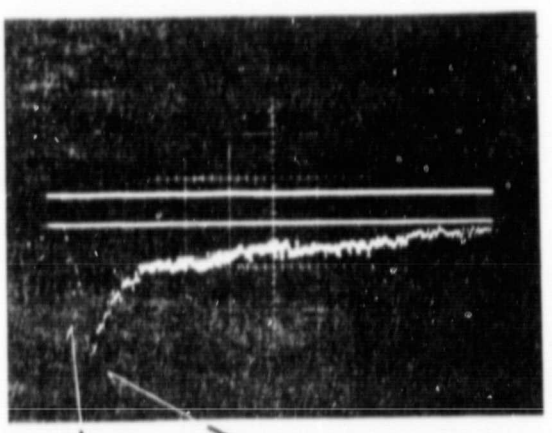

H_2 at 0.5 Torr
0.5 μsec / div

FIG. 8 PHOTOELECTRIC SIGNAL OF CONTINUUM (6980 Å) BEHIND THE REFLECTED SHOCK

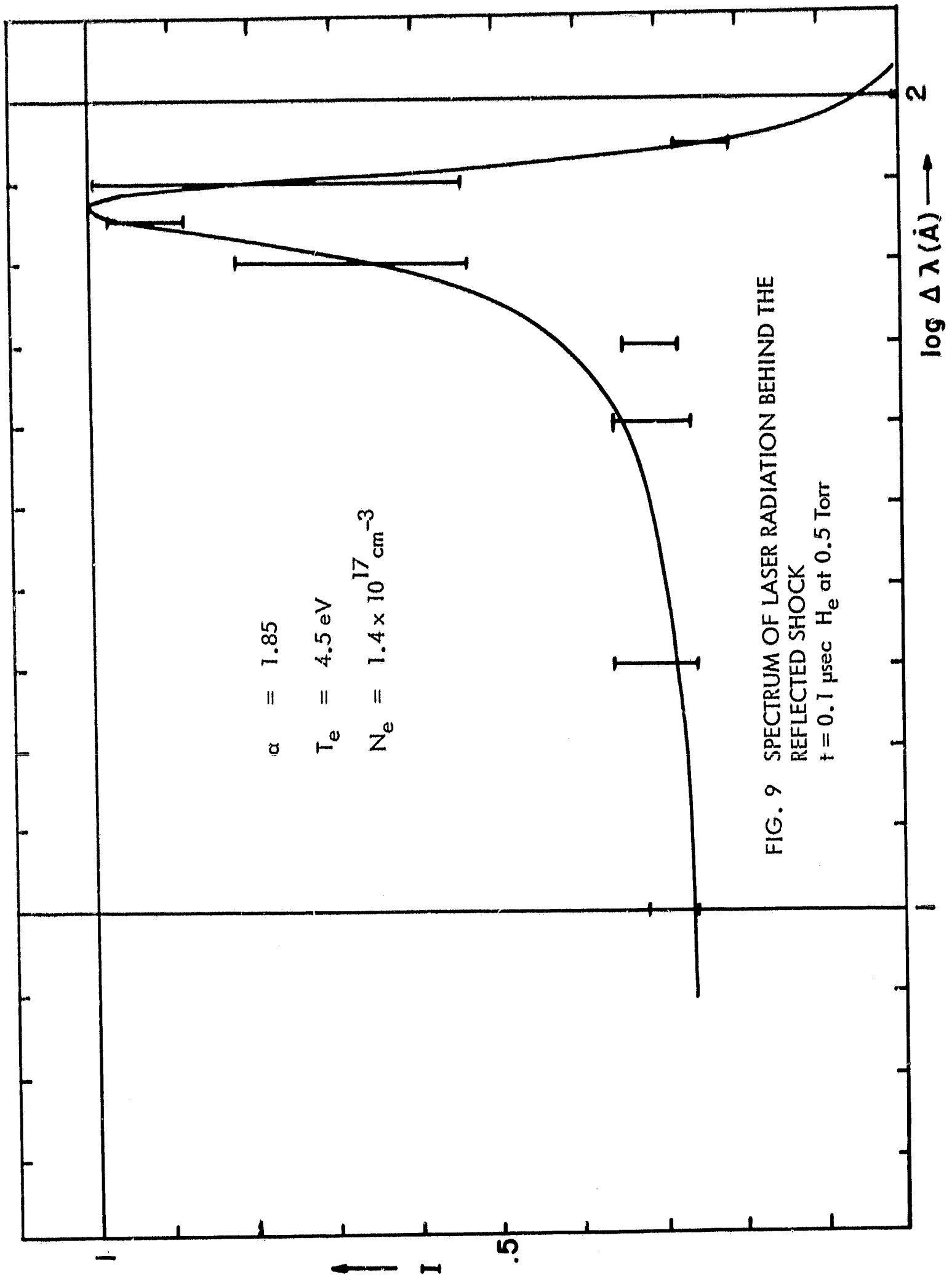

FIG. 9 SPECTRUM OF LASER RADIATION BEHIND THE REFLECTED SHOCK
t = 0.1 μsec H_e at 0.5 Torr

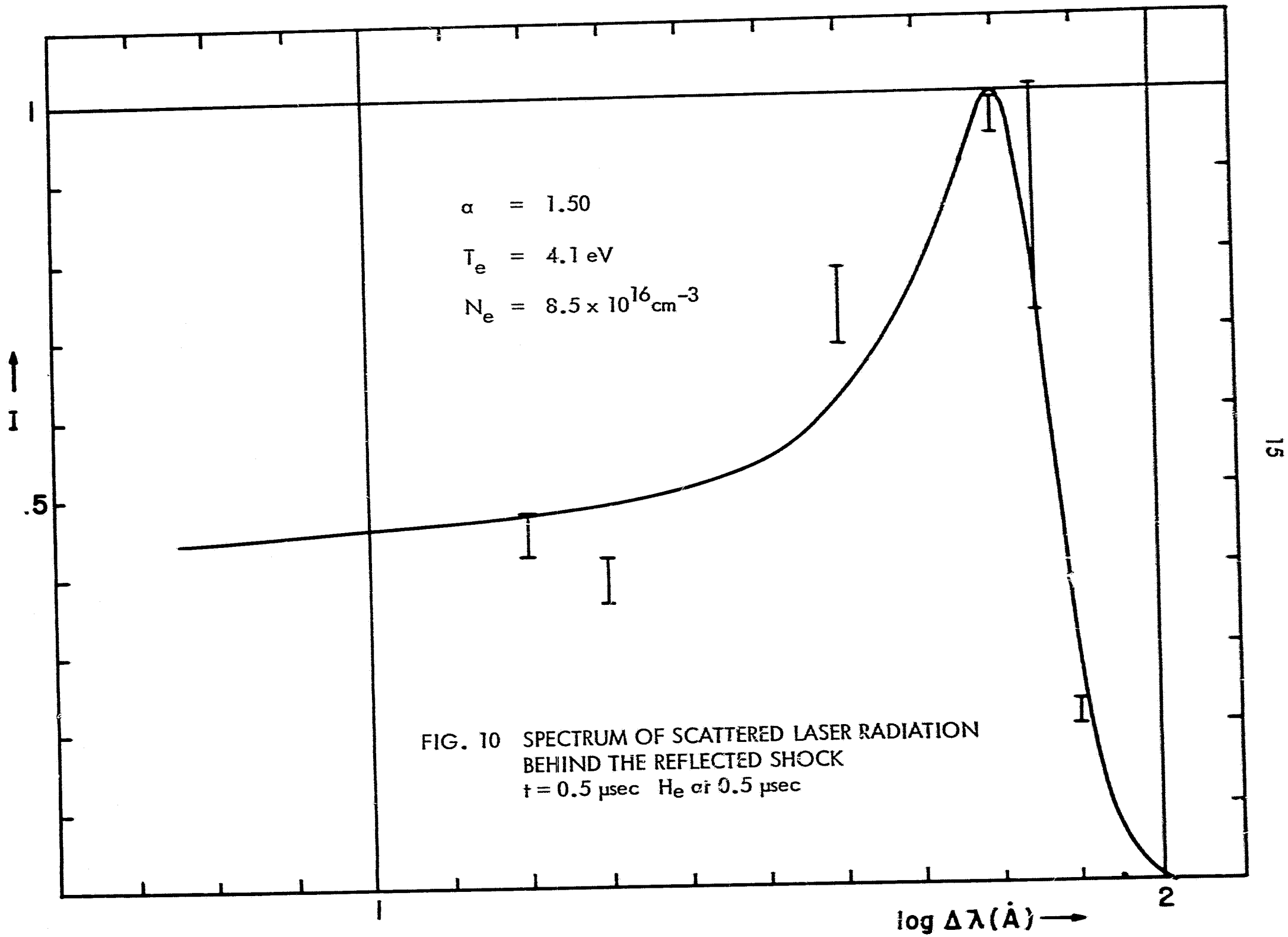

FIG. 10 SPECTRUM OF SCATTERED LASER RADIATION BEHIND THE REFLECTED SHOCK
t = 0.5 μsec H_e at 0.5 μsec

REFLECTED SHOCK, 0.5 TORR He

TIME	LASER SCATTERING Te	Ne	SPECTROSCOPIC Te
0.1 μsec	4.5 eV ± 10%	$1.4 \times 10^{17} cm^{-3}$ ± 10%	3.7 eV ± 15%
0.5 μsec	4.1 eV ± 10%	$8.5 \times 10^{16} cm^{-3}$ ± 10%	3.5 eV ± 15%
1.0 μsec	4 eV ± 10%	$7 \times 10^{16} cm^{-3}$ ± 10%	3.4 eV ± 15%

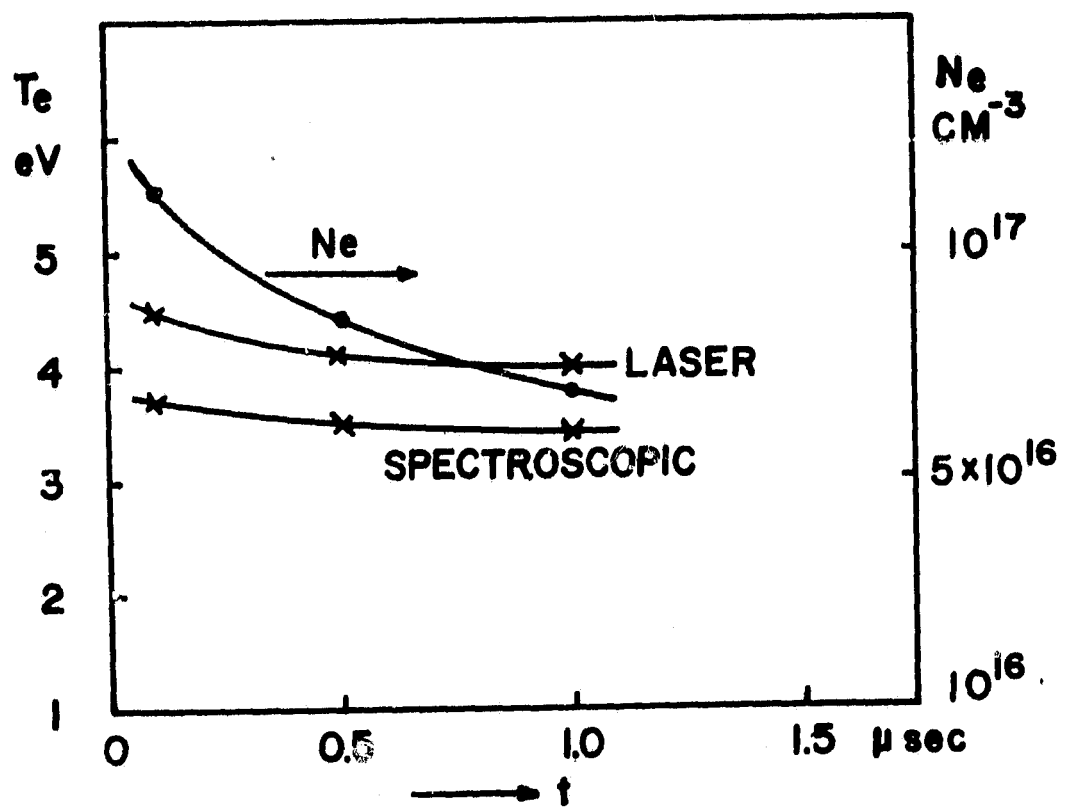

FIG. 11 ELECTRON DENSITY AND TEMPERATURE BEHIND THE REFLECTED SHOCK

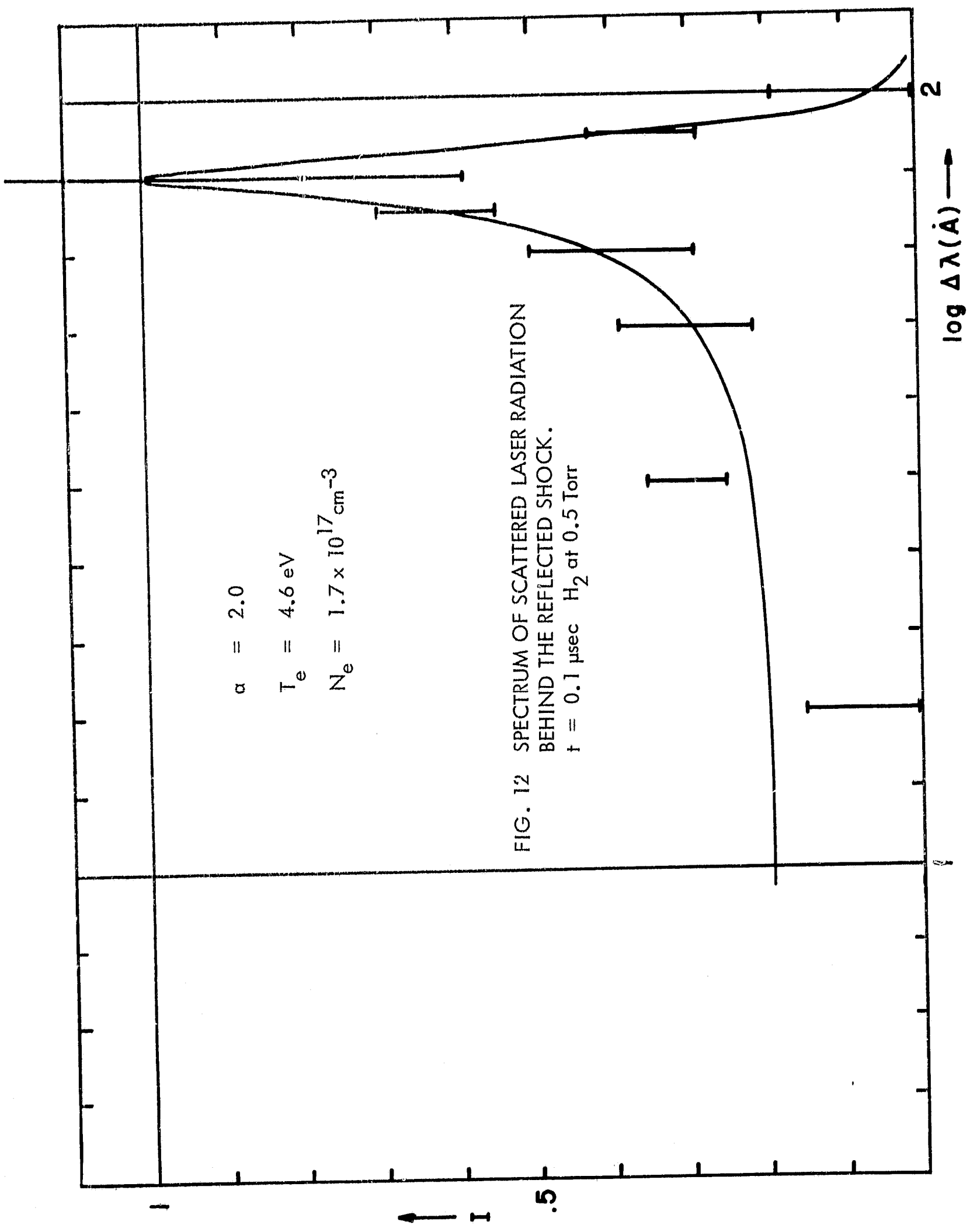

FIG. 12 SPECTRUM OF SCATTERED LASER RADIATION
BEHIND THE REFLECTED SHOCK.
t = 0.1 μsec H_2 at 0.5 Torr

would make the spectroscopic temperature lower than the scattering temperature as obtained in this experiment and so would the latter explanation because the value obtained from scattering is essentially the temperature of a small portion of plasma (0.1 mm x 3 mm) at the tube axis whereas the spectroscopic temperature is the average value along the entire tube diameter (2.5 cm). It is known[8] that there exists a cold boundary layer near the walls of T-tube. In order to see this contribution to the temperature difference, the electron temperature near the tube wall is measured by the laser scattering method for reflected shock in helium. The result is shown in Figure 13. One does see, as expected, a tendency of a lower temperature near the tube wall although the difference is the within the estimated error.

D. Summary

In summary, the laser scattering method is used to determine the temperatures and densities of the plasma behind the shock wave produced in a T-tube. It was found that this method gives accurate values of plasma parameter which are well resolved in space and in time. Further reduction in the experimental uncertainty may be achieved by using a polychromator for the scanning of the entire spectral profile with a single shot. Another important fact is that an independent measurement of the electron temperature has given agreement with the temperature obtained from the spectral line intensity ratio measurement within the experimental accuracy of $\pm$ 15 percent which is well below the factor of two claimed by others[3]. This implies that the thermal equilibrium assumption made for the spectroscopic temperature measurement is a satisfactory one for the condition of this experiment and also for previous measurements[5] on coaxial accelerator plasma where the plasma condition is similar to that of the T-tube.

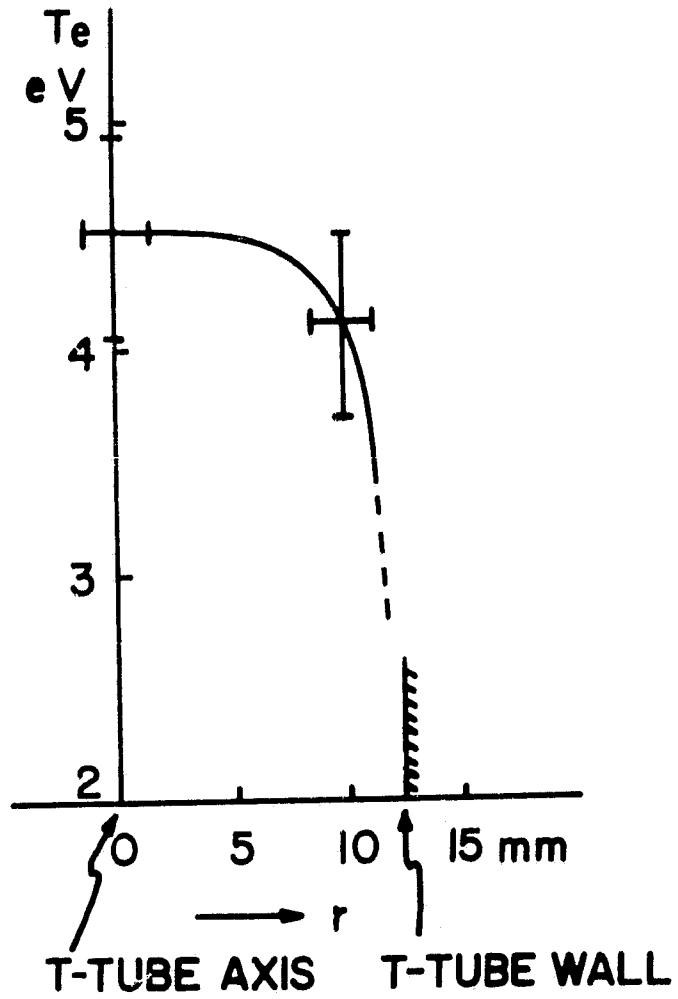

FIG. 13 TEMPERATURE PROFILE

II. Drift Instabilities in Two Component Plasmas

A. Introduction

In an earlier paper[9], a formulation was presented for the study of plasma oscillations in bounded and unbounded plasmas with transverse density variations in a strong axial magnetic field. Detailed calculations were made on the effects of density inhomogeneity and boundary on the oscillation characteristics of stationary plasmas and the stability of two identical counterstreaming electronic plasmas[9,10]. Since the validity of the formulation has been supported by relevant experiments[11,12], it is felt that further consequences of the theory should be revealed. The purpose of this paper is to report the results of an investigation on the stability of plasmas having two Maxwellian components of different drift velocities and temperatures under experimentally realistic conditions. This problem is of considerable interest in thermonuclear research and in the infinite and homogeneous limit, has been studied by Buneman[13], Jackson[14] and Jackson[15]. Using the formulation developed in Ref. 9, we are able to give general expressions for the velocity thresholds, maximum unstable wavenumber, and the number of unstable modes in a system. In conjunction with the geometrical parameters given earlier[9,10], the formulas can be used to study the instability under a variety of conditions. It is seen that the instability depends sensitively on both the geometry and the temperature ratio of the two components. The main features are illustrated by specializing to the case of a proton-electron plasma bounded by a conducting cylinder.

B. Mathematical Formulation

Stability Criterion

We are concerned with electrostatic instabilities in plasmas confined by a strong

axial magnetic field so that transverse motions of the charged particles can be neglected. They may or may not be bounded by a conducting wall at a radial distance d from the center. The zero-order density is assumed to be uniform in the axial direction but can have any arbitrary profile in the transverse direction. The dispersion relations for electrostatic oscillations are then given by[9]

$$\sum_j \frac{\omega^2_{pj}}{k^2} \int_{-\infty}^{\infty} \frac{\partial f_{oj}/\partial v}{v - \omega/k}\, dv = \nu_n(k,d,a); \qquad (1)$$

$$n = 0, 1, 2 \text{ ----- },$$

where the ν_n's are the eigenvalues of a Sturm-Liouville problem and subscript n denotes the nth mode. d is the radial dimension of the system and the parameter a characterizes the radial plasma density inhomogeneity. ω_{pj} is the plasma frequency of species j at the position of maximum density.

The left-hand side is the usual plasma dispersion function and can therefore be treated by the familiar techniques used in the theory of homogeneous plasmas. Adapting Jackson's[14] procedure, we arrive at the following instability criterion:

$$\sum_j \frac{\omega^2_{pj}}{k^2} P \int_{-\infty}^{\infty} \frac{G_j(v)\, dv}{v - x} = \nu_n(k,d,a) \qquad (a)$$

where x is determined from (2)

$$\omega^2_{pj} G_j(x) = 0 \qquad (b)$$

P in Eq. (2a) denotes the principal value and $G_i(v) = \partial f_{oi} / \partial v$.

Previous studies[9,10] of Eq. (2) were confined to two identical counterstreaming electronic plasmas in which the ionic mass was assumed to be infinite and only the electron dynamics needed be considered. In this paper, we are concerned with plasmas with electrons and ions of different drift velocities and temperatures. The velocity distributions are assumed to be Maxwellian. As pointed out by Buneman[13], the instability of such two-component current-carrying plasmas requires the treatment of the dynamics of both species. Equation (2) for this case therefore takes the form

$$\frac{\omega_{pe}^2}{k^2} P \int_{-\infty}^{\infty} \frac{G(v)\, dv}{v - x} = V_n(k,d,a) \qquad (a)$$

$$G(x) = 0 \qquad (b) \qquad (3)$$

where

$$G(v) = (1/n_o) \left[\partial f_{oe} \partial v + (m_e/m_i) \partial f_{oi} / \partial v \right]$$

$$= -\frac{1}{\sqrt{2\pi}\, \bar{v}_e^2} \left[\frac{(v - u_e)}{\bar{v}_e} \exp\left\{ -\frac{(v - u_e)^2}{2 \bar{v}_e^2} \right\} + \frac{T_e}{T_i} \left(\frac{v - u_i}{\bar{v}_i^2} \right) \exp\left\{ \frac{-(v - u_i)^2}{2 \bar{v}_i^2} \right\} \right] \qquad (4)$$

In Eq. (4), $T_i = \frac{1}{2} m_i \bar{v}_i^2$ and is the kinetic temperature of species i. The symbols v_i, u_i and m_i denote the thermal velocity, drift velocity and mass of species i respectively. n_o is the maximum number density.

Following Jackson[14], we let

$$w_1 = (u_e - v)/\bar{v}_e, \qquad w_2 = (v - u_2)/\bar{v}_i. \qquad (5)$$

Then the velocity difference

$$U = (u_e - u_i) = \bar{v}_e \left(w_1 + \sqrt{\frac{m_e\ T_i}{m_i\ T_e}}\ w_2\right) \tag{6}$$

and

$$G(w_1, w_2) = \frac{1}{\sqrt{2\pi}\ \bar{v}_e^{\,2}} \left[w_1 \exp(-0.5\ w_1^{\,2}) - \frac{T_e}{T_i} w_2 \exp(-0.5\ w_2^{\,2}) \right] \tag{7}$$

Substituting (5) and (7) into (3), the stability criterion for the nth mode can be shown to be

$$\beta^2\ V_n(k,d,a) = w_1^{\,2}\ Y(w_1/\sqrt{2}) + \theta\ w_2^{\,2}\ Y(w_2/\sqrt{2}) - (1+\theta) \tag{8}$$

(a)

and w_1, w_2 are evaluated at $v = x$ where $G(x) = 0$ (b)

In equation (8),

$$Y(x) = \frac{\exp(-x^2)}{x} \int_o^x \exp(y^2)\, dy \tag{9}$$

$$\theta = \frac{T_e}{T_i}\ ;\ \beta = k\bar{v}_e/w_{pe} = k/k_D \tag{10}$$

where k_D is the electron Debye wavenumber at the position of maximum density. The condition $G(x) = 0$ is satisfied when

$$w_1\ \exp(-0.5\ w_1^{\,2}) = \theta\ w_2\ \exp(-0.5\ w_2^{\,2})$$

or

$$\ln w_1 - 0.5\ w_1^{\,2} = \ln\theta + \ln w_2 - 0.5\ w_2^{\,2} \tag{11}$$

Equation (11) is easily solved graphically. For each temperature ratio θ, there is a functional relationship between w_1 and w_2. Hence we can write

$$w_2 = f(w_1)$$

For the special case of equal temperatures, $\theta = 1$ and $w_2 = w_1$.

The relative velocity U can be found from equation (6) for a given value of w_1. Thus the stability criterion can be written in the form

$$\beta^2 \nu_n(d,a,k) = F(U/\bar{v}_e, \theta) \tag{12}$$

We see in equation (12) that the geometrical factors affect the instability through ν_n while the temperature ratio affects it through the function F.

Velocity Thresholds

For a given temperature ratio θ and a given geometry specified by ν_n, equation (12) gives the maximum unstable wavenumber as a function of the relative drift velocity U. The function F in (12) is a superposition of two functions of the form Y defined by (9), the behaviour of which is well known[14]. The important feature to note is that, Y, and hence F, has a finite zero, a maximum, and a zero at infinity.

For the left hand side, it was shown previously[9] that the eigenvalues ν_n posseses the property that

$$\lim_{k \to 0} k^2 \nu_n = \epsilon_n^2 > 0 \qquad \text{for a bounded and /or inhomogeneous plasma} \tag{13}$$

There are thus two velocity thresholds at which waves with zero wavenumber begin to grow. The lower threshold, denoted by U_{o1}, is the minimum relative velocity required for instability. The upper threshold, denoted by U_{o2}, gives the value of drift velocity difference beyond which no growing wave is possible. These thresholds are given by the intersection of the line $(\frac{\epsilon_n^2}{k_D^2})$ with F, namely,

$$(\epsilon_n^2 / k_D^2) = F(U/\bar{v}_e, \theta) \tag{14}$$

An analytical but approximate expression for the upper velocity threshold U_{o2} can be obtained by noting that for large values of $w_1, w_1 \cong w_2 = w$. Substituting this in equations (8) and (14), we obtain

$$1 + \theta + \frac{\epsilon_n^2 \bar{v}_e^2}{\omega^2_{pe}} = (1 + \theta)\, w^2\, Y(w/\sqrt{2}) \tag{15}$$

For large w,

$$w^2 Y(w/\sqrt{2}) = 1 + 1/w^2 + 3/w^4 + 0(1/w^6) \tag{16}$$

Taking only the first three terms, (15) becomes

$$w^4\, \epsilon_n^2\, v_e^2 / \omega^2_{pe} = w^2 (1 + \theta) + 3 (\theta + 1),$$

of which the solution is

$$W = \frac{\omega_{pe}}{\epsilon_n \bar{v}_e} \left[\frac{1}{2}(1+\theta) + \left\{ \frac{1}{4}(1+\theta)^2 + 3(1+\theta) \frac{\epsilon_n^2 \bar{v}_e^2}{\omega_{pe}^2} \right\}^{\frac{1}{2}} \right]^{\frac{1}{2}} \tag{17}$$

For the usual case where $m_i >> m_e$, e.g. in a proton-electron plasma, $U/\bar{v}_e \simeq w$ from equation (6) and equation (17) gives the upper velocity threshold $U_{o2}/\bar{v}_e$ of the nth mode as a function of geometry and temperature ratio.

Number of Unstable Modes

As pointed out in an earlier paper[10], a bounded and/or inhomogeneous plasma can in general support several unstable modes of the two-stream instability. We wish here to investigate the dependence of the number of unstable modes on the temperature ratio. The eigenvalues ν_n can in general be expressed as [10]

$$\nu_n = 1 + a_n (Q/\beta) + \sigma_n (Q/\beta)^2 \tag{18}$$

where

$$Q = \bar{v}_e/d\,\omega_{pe} = L_D/d = 1/(k_D d) \text{ and } L_D \text{ is the electron Debye length} \tag{19}$$

at the position of maximum density

Thus

$$\epsilon_n^2/k_D^2 = \sigma_n Q^2. \tag{20}$$

Using (20), equation (15) can be written as

$$\sigma_n Q^2 = F(\theta, U/\bar{v}_e) \tag{21}$$

Let the maximum value of $F(\theta, U/\bar{v}_e)$ be denoted by F_{max}. Equation (21) implies that for a given radial dimension of the system as specified by Q, modes for which $\sigma < F_{max}/Q^2$ are unstable and those with $\sigma > F_{max}/Q^2$ are damped. If Q_n is the maximum value which Q can take in order to excite modes up to the nth order, then

$$Q_n = (F_{max}/\sigma_n)^{1/2} \tag{22}$$

Note that F_{max} and hence Q_n is a function of the temperature ratio θ.

The parameters σ_n and ϵ_n depend on the diameter of the system and the radial density profile. In addition to these two factors, the eigenvalues ν_n depend also on the wavenumber. In an earlier paper[10], these parameters have been given for several configurations. Equations (14), (16), and (22) can therefore be used to determine the stability of the plasma under a variety of conditions. The main features are illustrated in the following section by considering the case of a proton-electron plasma uniformly filling a conducting cylinder.

Uniform Proton-Electron Plasma Column Bounded by a Conducting Cylinder

To illustrate the main features of the instability, we specialize to the case of a uniform proton-electron plasma column bounded by a conducting cylinder of radius d. For circularly symmetric modes, the eigenvalues are given by[10]

$$\nu_n = 1 + (Q/\beta)^2 \alpha^2_{on} \tag{23}$$

where α_{on} is the nth root of $J_o(x)$. For example

$$\alpha_{o1} = 2.41$$

$$\alpha_{o2} = 5.52$$

$$\alpha_{o3} = 8.65 \qquad \text{etc.}$$

It follows from (23) that

$$\epsilon_n^2 = \lim_{k \to 0} k^2 \nu_n = Q^2 k_D^2 \alpha^2_{on}$$

Hence

$$(\epsilon_n^2/k_D^2) = Q^2 \alpha_{on}^2 \tag{24}$$

and

$$\sigma_n = \alpha_{on}^2$$

Using the above parameters, we can compute Q_n as a function of n with the temperature ratio θ as a parameter. The results are given in Table I. It is seen that Q_n increases as θ increases. This means that for a given geometry as specified by Q, the number of unstable modes increases as the temperature ratio increases. For example, let us take $Q = 0.1$, i.e. the radius of the cylinder is ten time the electron Debye length. Then modes for which $Q_n > 0.1$ are unstable and those with $Q_n < 0.1$ are damped. From Table I, the number of unstable modes which the system can support is easily found as a function of θ. This is shown in Table II. For example, when $\theta = 1$, only the lowest two modes are unstable. The number increases to four when $\theta = 10$.

The lowest mode ($n = 0$) is the one of the greatest interest since it determines the stability of the system. Again taking $Q = 0.1$, we have

$$\nu_o = 1 + 0.058/\beta^2$$

$$\frac{\epsilon_o^2}{k_D^2} = 0.058 \tag{25}$$

For a proton-electron plasma,

	Q_n					
n	$T_e/T_i=1$	$T_e/T_i=2$	$T_e/T_i=4$	$T_e/T_i=6$	$T_e/T_i=8$	$T_e/T_i=10$
0	0.318	0.373	0.448	0.505	0.550	0.602
1	0.138	0.163	0.195	0.219	0.240	0.262
2	0.088	0.104	0.125	0.140	0.153	0.167
3	0.065	0.076	0.092	0.013	0.113	0.123
4	0.051	0.060	0.072	0.081	0.089	0.097
5	0.042	0.050	0.060	0.064	0.074	0.080

Table I. The parameter Q_n as a function of T_e/T_i for a proton-electron plasma bounded by a conducting cylinder of diameter twenty times the electron Debye length.

T_e/T_i	Number of unstable modes
1	2 (n = 0, 1)
2	3 (n = 0, 1, 2)
4	3 (n = 0, 1, 2)
6	4 (n = 0, 1, 2, 3)
8	4 (n = 0, 1, 2, 3)
10	4 (n = 0, 1, 2, 3)

Table II. Number of unstable modes as a function of T_e/T_i for a proton-electron plasma bounded by a conducting cylinder of diameter twenty times the electron Debye length.

$$m_e/m_i = 1/1836$$

$$U/\bar{v}_e = (w_1 + 0.0233\, w_2/\theta^{\frac{1}{2}}) \tag{26}$$

The velocity thresholds are determined from

$$0.058 = F(\theta, U/\bar{v}_e) \tag{27}$$

The range of unstable wavenumber is given by

$$\beta^2 + 0.058 = F(\theta, U/\bar{v}_e) \tag{28}$$

For each θ, there is a maximum β occuring at some value $U/\bar{v}_e$.

The dependence of the lower velocity threshold U_{o1}, the upper velocity threshold U_{o2}, and the maximum normalized unstable wavenumber β_{max} on the temperature ratio are illustrated in Figs. 14-16.. It is seen that in all three cases, the dependence on θ is marked.

C. Concluding Remarks

We have present general formulas for the study of the Buneman instability of two-component plasmas under a variety of conditions. It is seen that the instability is sensitively dependent on both the geometry and the temperature ratio of the two components. The main features have been illustrated by specializing to the case of a uniform plasma column bounded by a conducting cylinder. For other configurations of the same class, i.e. transversely bounded and/or having arbitrary density profiles, the qualitative nature of the instability is similar. Quantitative information of the instability can be obtained by simply using the eigenvalues γ_n for the configuration in question and substituting them into the formulas given.

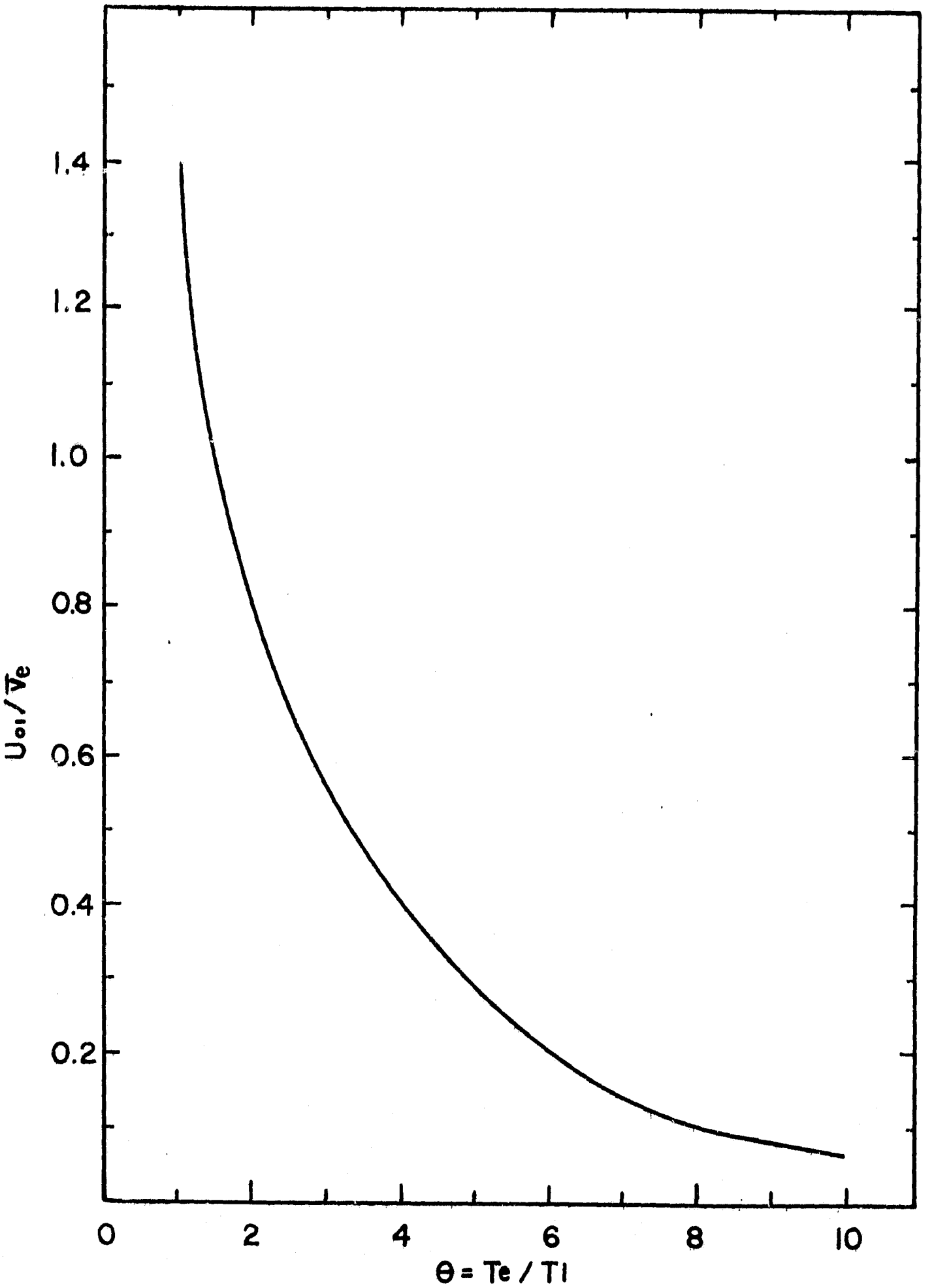

FIG. 14 DEPENDENCE OF THE NORMALIZED LOWER VELOCITY THRESHOLD $U_{01}/\bar{v}_e$ ON T_e/T_i FOR A PROTON-ELECTRON PLASMA BOUNDED BY A CONDUCTING CYLINDER OF DIAMETER TWENTY TIMES THE ELECTRON DEBYE LENGTH

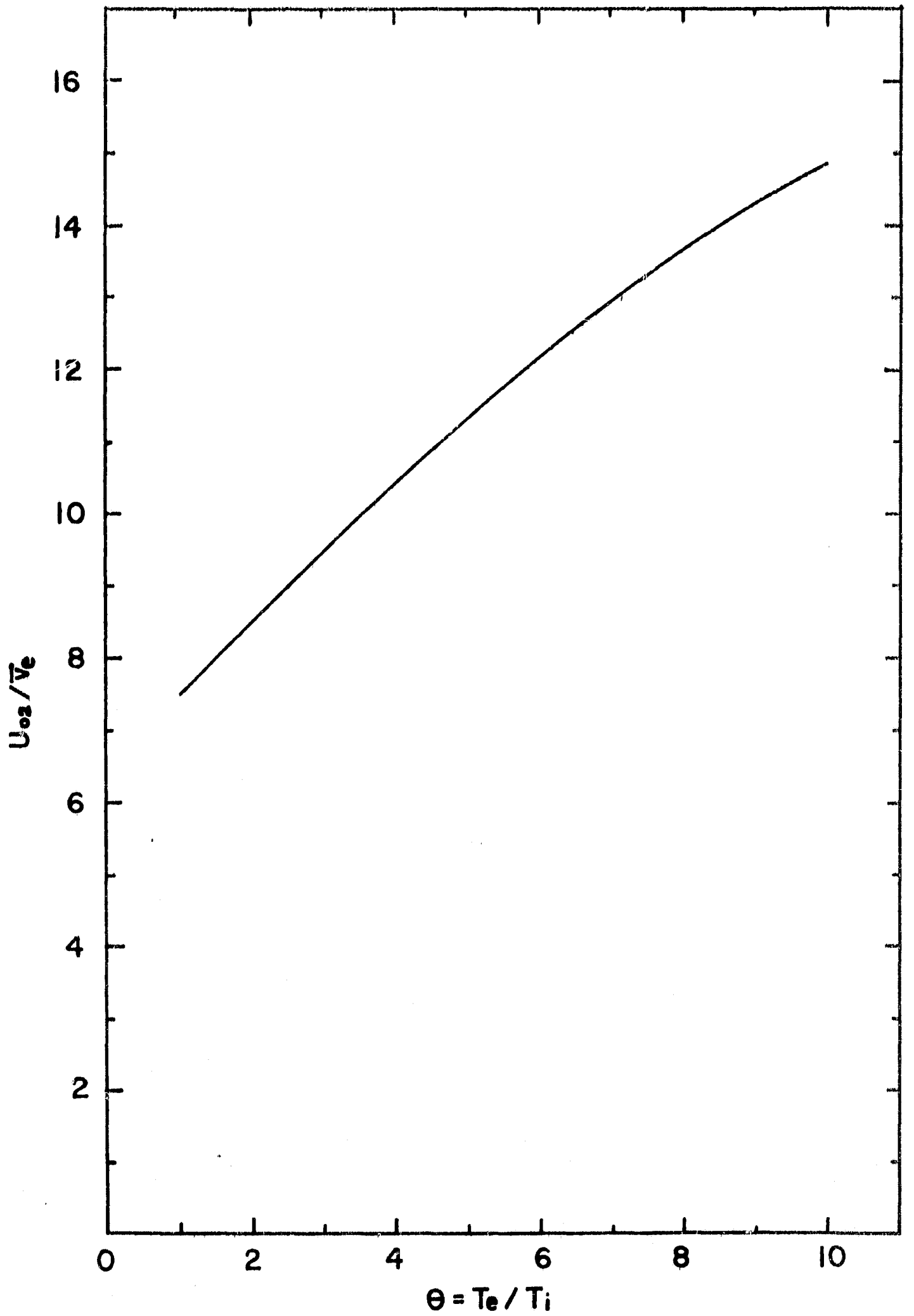

FIG. 15 SAME AS FIG. 14 EXCEPT FOR THE NORMALIZED UPPER VELOCITY THRESHOLD $U_{o2}/\bar{v}_e$

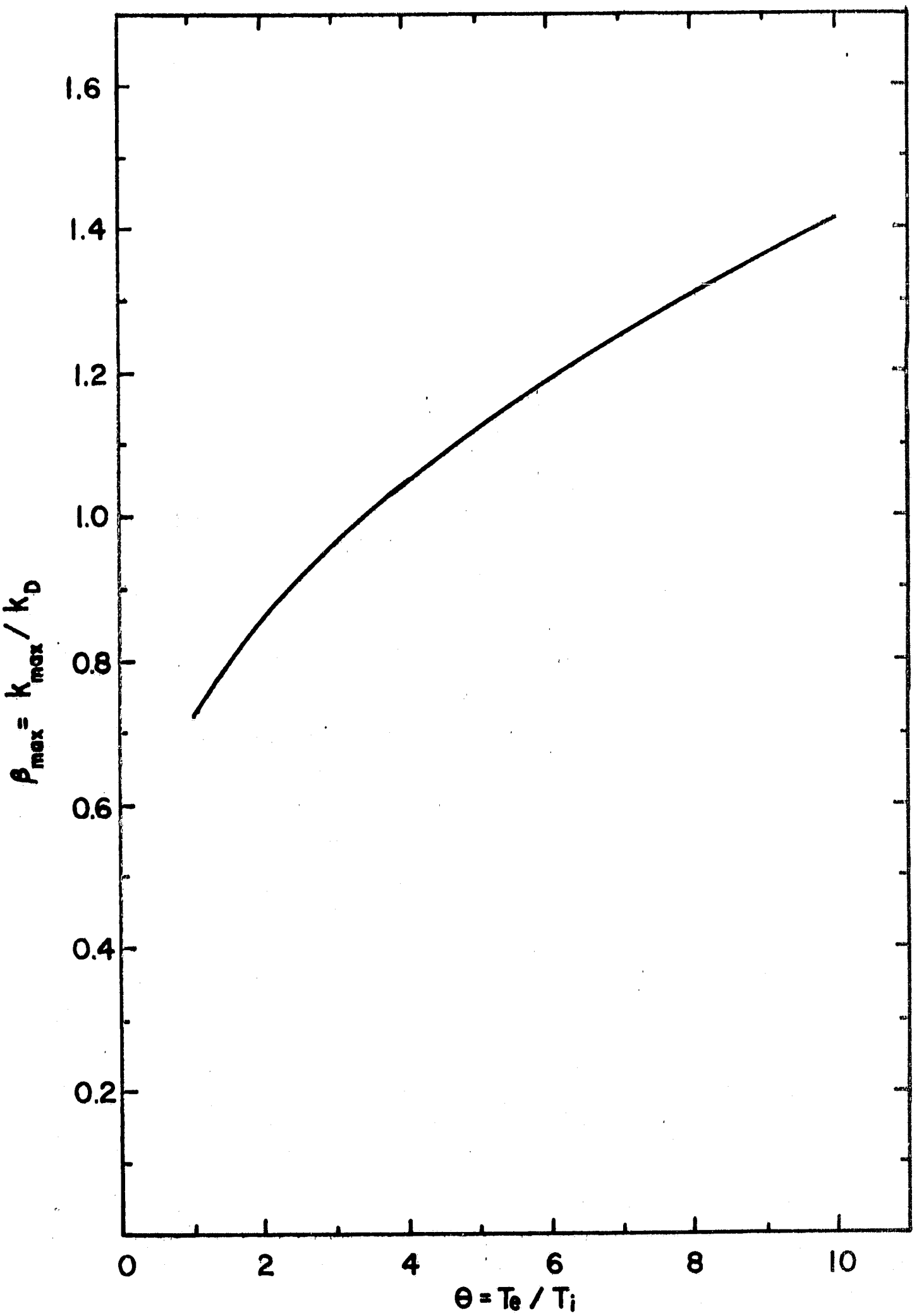

FIG. 16 SAME AS FIG. 14 EXCEPT FOR THE NORMALIZED MAXIMUM UNSTABLE WAVENUMBER β_{max}

The method of finding the eigenvalues has been dealt with in detail in earlier papers[9,10]. Finally, it should be pointed out that despite their generality, the formulas are unusually simple and the calculations involved require no more than a slide rule and a table of the function Y(x).

REFERENCES

1. E.A. McLean, C.E. Faneuff, A.C. Kolb and H.R. Griem, Phys. Fluids, 3, 843 (1961).

2. R.C. Isler and D.E. Kerr, Phys. Fluids 8, 1176 (1965).

3. K.K. Eckerle and R.W.P. McWhirter, Phys. Fluids 9, 81 (1966).

4. H.R. Griem, Plasma Spectroscopy (McGraw-Hill Book Co., Inc., New York, 1964).

5. T.N. Lie, A.W. Ali, E.A. McLean and A.C. Kolb, Phys. Fluids 10, 1545, (1967).

6. E.T. Gerry and R.M. Patrick, Phys. Fluids 8, 208, (1965).

7. Wilhelm H. Kegel, "Graphs for the Determination of Plasma Parameters by Light Scattering Experiments, Institute for Plasma Physics Report IPP 6/34 (1965) (in German).

8. E.A. McLean and S.A. Ramsden, Phys. Rev. 140, A1122, (1965).

9. K.F. Lee, J. Appl. Phys. 38, 235 (1967).

10. K.F. Lee, J. Appl. Phys. 38, 2172 (1967).

11. K.F. Lee, J. Appl. Phys. 38, 3787 (1967).

12. K.F. Lee, J. Appl. Phys. 38, 4543 (1967).

13. O. Buneman, Phys. Rev. Letters 1, 8 (1958).

14. J.D. Jackson, J. Nucl. Energy C1, 171 (1960).

15. E.A. Jackson, Phys. Fluids 3, 786 (1960).

PROJECT REFERENCES

1. "Diagnostics of Accelerating Plasma" Research Proposal for NASA Research Grant NGR-09-005-025, Feb. 1965.

2. "Spectroscopic Study of a Coaxial Plasma Gun", Bulletin 10 523, American Physical Society Meeting in Washington, D.C. April 26-29, 1965.

3. "Diagnostics of Accelerating Plasma" Part V, 102, Fifth NASA Intercenter Conference on Plasma Physics in Washington, D.C., May 24-26, 1966.

4. "First Semi-Annual Progress Report for the period March 1 - Aug. 31, 1966, Research Grant NGR-09-005-025. Report No. 66-010, Department of Space Science & Applied Physics, Catholic University of America, Washington, D.C.

5. "Electric Polarity Effect in Coaxial Plasma Accelerator", Paper 7C-1, Eighth Annual Meeting on Plasma Physics of American Physical Society, Boston Nov. 2-5, 1966.

6. "Plasma State in Coaxial Accelerator", Physics of Fluids 10 1545, 1967.

7. Second Semi-Annual Progress Report for the period September 1, 1966 - Feb. 28, 1967, Research Grant NGR-09-005-025, Report No. 66-021, Department of Space Science and Applied Physics, Catholic University of America, Washington, D.C.

8. "Magnetohydrodynamic Shock Wave Structure" by C.K. Liu, (Ph.D. Thesis 1967), Report No. 67-028, Department of Space Science and Applied Physics, Catholic University of America, Washington, D.C.

9. "Studies of Current Sheet in a Coaxial Plasma Accelerator" paper No. 67-658, AIAA Electric Propulsion and Plasmadynamics Conference, Colorado Springs, Sept. 11-13 1967.

10. "Pre-ionization Phenomena in Pulsed Plasma Accelerator" paper E5, Proc. APS Topical Conference on Pulsed High-Density Plasmas, Los Alamos, Sept. 19-22, 1967.

11. 3 rd Semi-Annual Progress Report for the period March 1, 1967 - August 31, 1967, Research Grant NGR-09-005-025, Report No. 67-029, Department of Space Science and Applied Physics, Catholic University of America, Washington, D.C.

12. 4th Semi-Annual Progress Report for the period Sept. 1, 1967 - Feb. 29, 1968, Research Grant NGR-09-005-025, Report No. 68-005, Department of Space Science & Applied Physics, Catholic University of America, Washington, D.C.

13. "Drift Instabilities in Confined Two-Component Plasmas", Journal of Applied Physics 39 3861 (1968).

14. "Local Thermal Equilibrium in Magnetically Driven Shock", Paper 3C-5 10th Annual Meeting on Plasma Physics, A.P.S., Miami, Fla., Nov. 13-16,(1968).